UCRL-CONF-153485

Photothermal multi-pixel imaging microscope

Christopher J. Stolz, Diane J. Chinn, Robert D. Huber, Carolyn L. Weinzapfel, and Zhouling Wu

This article was submitted
Boulder Damage Symposium XXXV
Annual Symposium on Optical Materials for High Power Lasers
Boulder, Colorado
September 22-24, 2003

December 1, 2003

U.S. Department of Energy

Lawrence
Livermore
National
Laboratory

Updated October 14, 2003

Photothermal multi-pixel imaging microscope

Christopher J. Stolz[a], Diane J. Chinn[a], Robert D. Huber[a], Carolyn L. Weinzapfel[a], and Zhouling Wu[b]
[a]University of California, Lawrence Livermore National Laboratory,
7000 East Avenue L-491, Livermore, CA 94550
[b]ValuTech Corporation, 5951 Corte Cerritos, Pleasanton, CA 94566

ABSTRACT

Photothermal microscopy is a useful nondestructive tool for the identification of fluence-limiting defects in optical coatings. Traditional photothermal microscopes are single-pixel detection devices. Samples are scanned under the microscope to generate a defect map. For high-resolution images, scan times can be quite long (1 mm^2 per hour). Single-pixel detection has been used traditionally because of the ease in separating the laser-induced topographical change due to defect absorption from the defect surface topography. This is accomplished by using standard chopper and lock-in amplifier techniques to remove the DC signal. Multi-pixel photothermal microscopy is now possible by utilizing an optical lock-in technique. This eliminates the lock-in amplifier and enables the use of a CCD camera with an optical lock in for each pixel. With this technique, the data acquisition speed can be increased by orders of magnitude depending on laser power, beam size, and pixel density.

Keywords: Photothermal microscopy, absorption, nondestructive testing, multilayer coating

1 INTRODUCTION

Fluence-limiting defects in optical coatings can be differentiated from benign defects with photothermal microscopy.[1-7] Defects with little photothermal signal survive significantly higher fluences than defects with high photothermal signal. In fact, a linear relationship has been demonstrated between photothermal signal and laser damage threshold.[2] Therefore, one can identify fluence-limiting defects for further characterization such as cross-sectioning with a focused ion beam for determining the unique geometrical and chemical characteristics of that particular defect.[8-9] Photothermal microscopy has also been used to demonstrate that absorptance of a defect is reduced after nodular ejection, a mechanism of laser conditioning.[3] Finally, photothermal microscopy has been used to identify defects that heat during laser exposure, yet are not visible with optical microscopy.[10-17]

Although photothermal microscopy has been demonstrated as a powerful tool for non-destructive laser damage threshold prediction, the use of these microscopes has been limited by very slow data acquisition speeds. Consequently, high resolution characterization of large areas has not been attempted. Unfortunately, damage testing small areas does not typically reveal the true laser-induced damage threshold of a large-area coating. For example, e-beam deposited transport mirrors at 1053 nm with a surface area of 3,000 cm^2 have roughly 1,000,000 micron-sized defects in a hafnia silica multilayer coating. Approximately 5,000 of these defects eject at 27 J/cm^2 (10-ns pulse length) as indicated by the presence of a plasma during laser conditioning. At the damage threshold of 38 J/cm^2 (10-ns pulse length), typically 1 to 6 damage sites occur. Therefore, to determine what makes these fluence-limiting defects unique from the other million defects on the full-aperture mirror, data sampling rates need to increase by several orders of magnitude from the current rate of 1 mm^2 per hour. One method of improving data acquisition speed is through the use of multi-pixel photothermal microscopy.

2 SETUP

A traditional photothermal system, illustrated in figure 1, is described in detail elsewhere.[2] In summary, the microscope has a chopped focussed pump beam that causes a transient thermal bump on a coated surface. The greater the thermal absorption of the coating or defect, the higher the amplitude of the thermal bump. The thermal bump diffracts a probe

beam causing a change in the magnitude of the signal on a position array detector. A lock-in amplifier is used to isolate the transient photothermal signal of the coating. A stage translates the sample to map the coating.

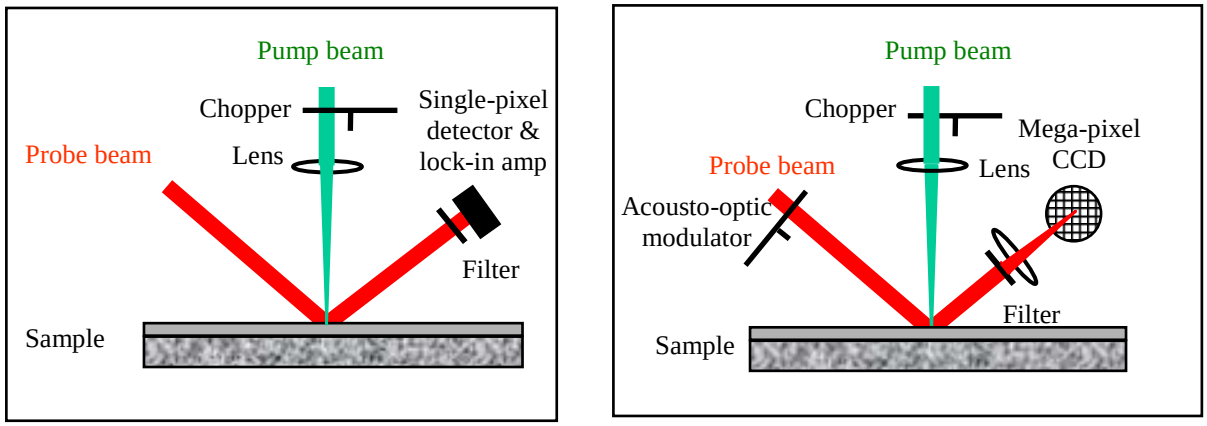

Fig. 1 Schematic of single-pixel (left image) and multi-pixel (right image) photothermal microscopes.

By modifying the probe beam and detector as illustrated in figure 1, the amount of data captured over a single location on the sample can be increased by several orders of magnitude thus enabling scanning large areas over reasonable time periods. The position array detector and lock-in amplifier are replaced with lock-in imaging[18] consisting of an acoustic modulator and spatial filter in the probe beam and a 2-D array detector (CCD camera). By modulating the pump and probe laser beam with the same modulation frequency, but with varying phase delay as illustrated in figure 2, both the amplitude and phase lock-in images Q_{amp} and Q_{phase}, respectively, can be computed during post-processing using the following relations:

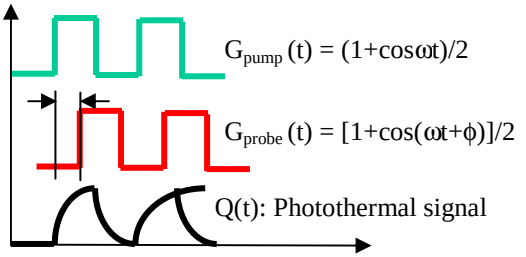

Fig. 2 Schematic of phase delay for quadrature detection.

$$Q_{amp} = \sqrt{(Q_0 - Q_{180})^2 + (Q_{90} - Q_{270})^2}$$

$$Q_{phase} = \tan^{-1}\left(\frac{Q_{90} - Q_{270}}{Q_0 - Q_{180}}\right)$$

Fig. 3 Photo of the multi-pixel photothermal microscope.

The amplitude signal, Q_{amp}, represents the difference in absorption between the defect and the coating. This absorption difference may be due to poor stoichiometry within the defect, standing-wave electric-field enhancement due to the defect geometry, or electronic defects.[19] This increase in absorption may lead to laser damage at higher fluences. The phase signal, Q_{phase}, gives information about the continuity of the defect and coating. Large phase differences are typical of significant thermal discontinuities at interfaces or poor thermal conductivity.

A few technical hurdles had to be overcome when assembling the microscope pictured in figure 3. To facilitate scanning vertically orientated 15-cm size substrates, the microscope was elevated thus making it more suspectable to vibration. More rigid fixturing was used to decrease the vibration of the system. A spatial filter

was installed in the probe beam to improve amplitude uniformity over the detector region. A telescope was installed in front of the camera to increase the resolution of the microscope and utilize a greater percentage of the pixels. Optical noise from fizeau fringes due to the uncoated parallel windows in the camera were eliminated by installing wedged coated windows to protect the cooled CCD from condensation.

3 EXPERIMENTAL RESULTS

3.1 Demonstration with "model" defects

In order to validate the optical lock-in technique, aluminum dots of various diameters were sputtered onto a glass surface. The high absorption of a metal disk on a low-absorbing glass substrate provided sufficient signal to be detected by the photothermal multi-pixel imaging microscope. The metallic dots were measured by both the single- and multi-pixel configuration as illustrated in figure 4. The data acquisition speed for the multi-pixel configuration was 50× faster than the single-pixel configuration. A disadvantage of the multi-pixel configuration is a greater amount of background noise. For highly-absorbing defect detection, the increased background noise is not significant, however, it is problematic for studying weakly absorbing defects. To overcome this limitation, a dual-head microscope could be configured with the multi-pixel configuration used to quickly identify defects and the single-pixel configuration used to create high-resolution defect images.

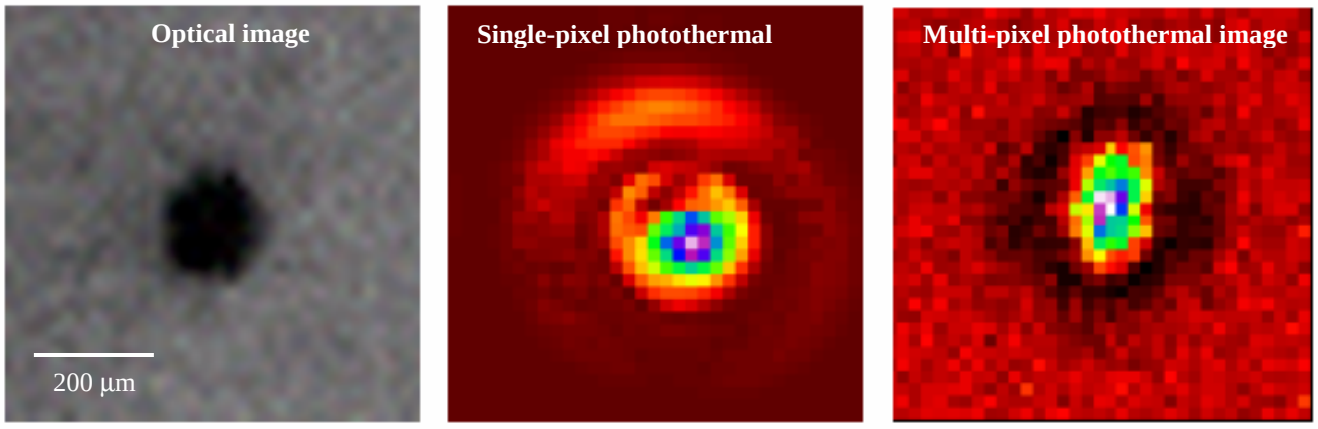

Fig. 4 High-resolution images of a "model" defect consisting of a 200-μm diameter sputtered aluminum dot. The single pixel data acquisition time was 35 minutes compared to only 3 minutes for the multi-pixel photothermal microscope.

The data acquisition speed of the multi-pixel photothermal microscope is limited by the integration and data transfer speed of the CCD camera. For this microscope an Apogee astronomical camera was used with a 40 second delay between images. Four images must be collected to calculate the photothermal amplitude signal. The laser power of the pump limits the size of the focused beam with sufficient fluence to create thermal bumps in the defects of interest as determined by previous photothermal studies. Currently, a 5 W laser is being used as the pump laser. This limits the area being pumped to approximately 200 μm by 200 μm, using a baseline of approximately 1 W/mm^2 of pump power needed to "activate" a defect. Many scans have been run with the magnification of the system set to image an area of the sample of approximately 0.5 mm × 0.5 mm. With this magnification, the 1024 × 1536 CCD array yields better than 2 pixels per micrometer in both the X and Y directions of the images. This resolution is much greater than that required to locate the defects of interest. However, the maximum pump size uses less than 20% of the available pixels, and so operating at a lower magnification would only decrease resolution without decreasing scan time. Therefore, a higher power laser is required to pump a larger area of the sample and thus increase the scanning speed.

A diffraction model of the photothermal response to an aluminum dot was created to compare the two different microscope configurations to theory. The diffraction model assumes a qaussian probe beam and a gaussian shaped lens resulting from heating of the aluminum absorber. Normalized profiles for single-point photothermal, multi-point

photothermal and the diffraction model are presented in figure 5. The higher noise in the multi-pixel image is evident, however, good agreement with theory occurs for both microscopes.

3.2 Demonstration with "real" coating defects

A coating sample was scribed with a diamond tip indenter to create a fiducial consisting of a grid pattern of 1 mm × 1 mm squares. The gridded sites were examined with an optical microscope to identify coating defect locations to compare with photothermal images. Both photothermal microscope configurations (single and multi-pixel) were used to generate photothermal images of the scribed regions. A comparison of the optical microscope and photothermal microscope images is illustrated in figure 6. Large absorbers appear in the left and right scribed boxes of the photothermal images. The SEM image does not show all of the defects that appear in the photothermal images. As with the case of the ideal defects, there is a greater amount of background noise in the images from the multi-pixel photothermal microscope. Therefore, the usefulness of this architecture is primarily in identifying highly absorptive defects over large areas at high speeds.

3.3 Demonstration over a large area

Photothermal microscopy over a square millimeter has been demonstrated by multiple groups.[7,10-17] High-resolution scans over a square centimeter has not yet been demonstrated until now as illustrated in figure 7. The interest of our group is in the "quick" identification of the highest absorbing defects within an optical coating. Typically at the onset of damage, only a few defects damage in a coating so are rare events. In order to find these fluence limiting defects, sufficient area must be interrogated.

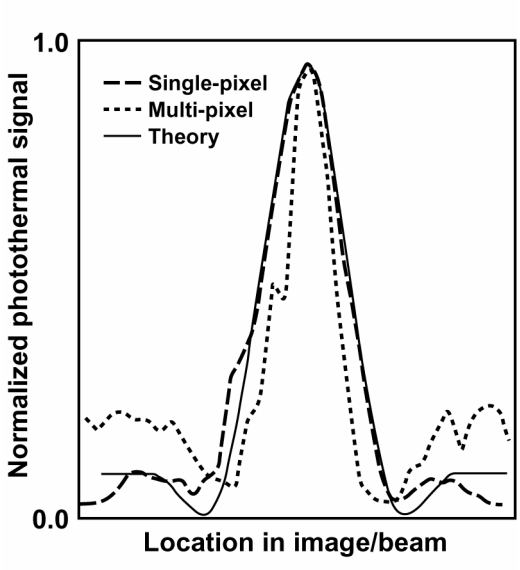

Fig. 5 Comparison of diffraction-based model of an aluminum absorber and actual measurements from photothermal microscopes in the single-pixel and multi-pixel configurations.

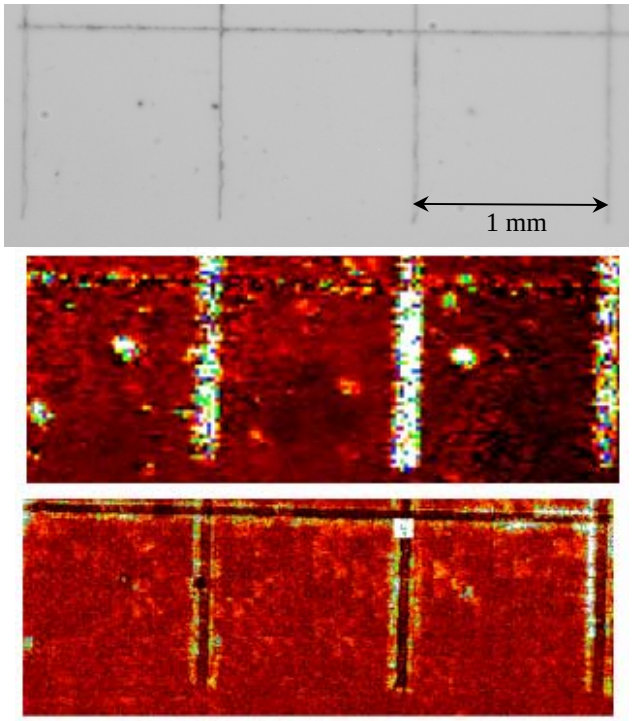

Fig. 6 Images of real coating defects within diamond scribed areas for fidiculization using an optical microscope (top), single-point photothermal microscope (middle), and multi-point photothermal microscope (bottom).

The multi-pixel photothermal microscope generates an enormous amount of data. Over a 1 cm^2 area and a pixel size of 0.25 μm^2, there are 400,000,000 pixels of data. In order to sort through all of this data, thresholding was done to ease visual location of the highest absorbing defects. Fiducilization by scribing the scanned area eased locating the defects under an optical microscope. For this particular high reflector coating, digs and dust (or contamination) were found to be the highest absorbing defects.

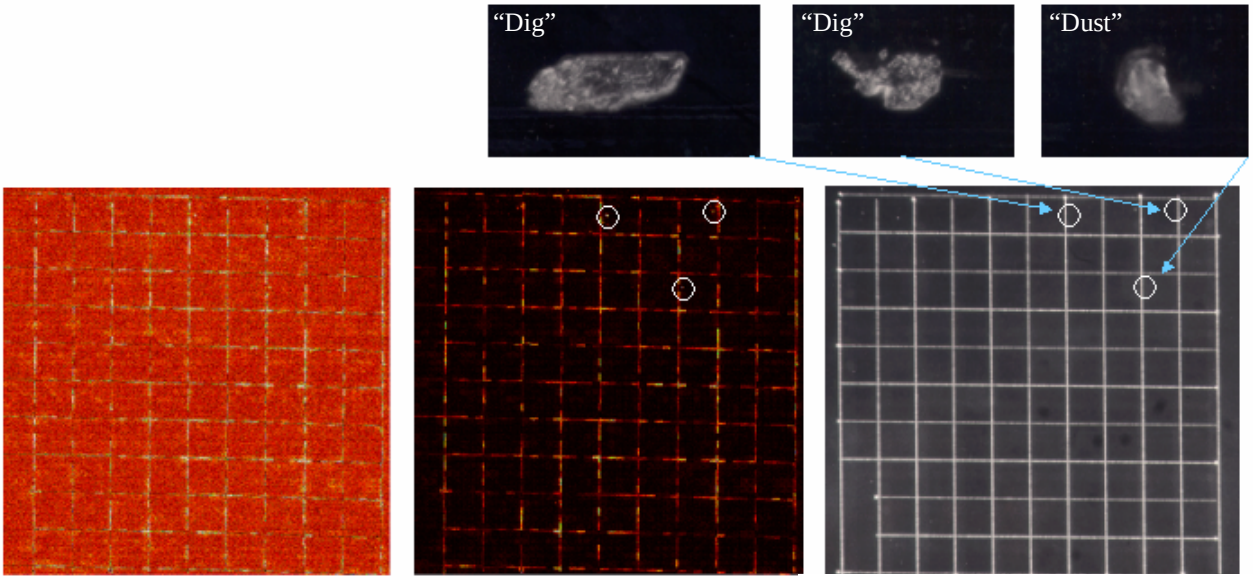

Multi-pixel photothermal image without thresholding

Multi-pixel photothermal image with thresholding

Optical image

Fig. 7 A 100 mm^2 area was mapped using multi-pixel photothermal scanning microscopy over a 24-hour period. The sample was scribed for fiducialization. The highest absorbing defects were either digs or pits in the coating and "dust" or a contamination particle that was removed during cleaning.

4 CONCLUSIONS

Photothermal microscopy is a powerful tool for non-destructive evaluation of coating defects that limit the laser resistance of multi-layer coatings. Unfortunately, the data acquisition speed for traditional single-pixel detection photothermal microscopes is prohibitively slow to study coating laser resistance over large areas. A new method using an optical lock-in technique has been demonstrated with a data acquisition speed of almost 100× greater that the single-pixel method. With a more energetic pump laser and a faster camera, data acquisition speeds of 10^5× greater than the single-pixel method could be achieved. Although higher background noise is evident in the multi-pixel configuration, this instrument is extremely useful for identifying highly absorbing defects that are believed to be the fluence-limiting defects of an optical coating. A dual-head system could be used to quickly identify the location of defects of interest with the multi-pixel configuration followed by subsequent slow scans over the defect with the single-pixel configuration for lower noise images.

5 AKNOWLEDGEMENTS

The authors would like to acknowledge the support of Andrea Flammini in preparing this manuscript and Mark McDaniel for assistance with the graphics. This work was performed under the auspices of the U. S. Department of Energy by the University of California, Lawrence Livermore National Laboratory under Contract No. W-7405-Eng-48.

REFERENCES

1. C. J. Stolz, J. M. Yoshiyama, Z. L. Wu, A. Salleo, J. Green, J., and R. Krupka, "Characterization of nodular and thermal defects in hafnia/silica multilayer coatings using optical, photothermal, and atomic force microscopy," in *Laser-Induced Damage in Optical Materials: 1997*, G. J. Exarhos, A. H. Guenther, M. R. Kozlowski, and M. J. Soileau, eds., Proc. SPIE 3244, 475-483 (1998).
2. Z. L. Wu, C. J. Stolz, S. C. Weakley, J. D. Hughes, and Q. Zhao, "Damage threshold prediction of hafnia -silica multilayer coatings by nondestructive evaluation of fluence-limiting defects," Applied Optics, Vol. **40**, 1897-1906 (2001).
3. A. B. Papandrew, C. J. Stolz, Z. L. Wu, G. E. Loomis, S. Falabella, "Laser conditioning characterization and damage threshold prediction of hafnia/silica multilayer mirrors by photothermal microscopy," in *Laser-Induced Damage in Optical Materials: 2000*, G. J. Exarhos, A. H. Guenther, M. R. Kozlowski, K. L. Lewis, and M. J. Soileau, eds., Proc. SPIE 4347, 53-61 (2001).
4. A. During, M. Commandre, C. Fossati, B. Bertussi, J. Y. Natoli, J. L. Rullier, H. Bercegol, and P. Bouchut, "Integrated photothermal microscope and laser damage test facility for in-situ investigation of nanodefect induced damage", Optics Express **11**, 2497-2501 (2003).
5. M. Reichling, A. Bodemann, and N. Kaiser, "Defect induced laser damage in oxide multilayer coatings for 248 nm," Thin Solid Films **320**, 264-279 (1998).
6. A. Bodemann, N. Kaiser, M. Reichling, E. Welsch, "Micrometer resolved inspection of defects and laser damage sites in UV high-reflecting coatings by photothermal displacement microscopy", J. Physique IV **4**, C7611-C7614 (1994).
7. A. Fornier, C. Cordillot, D. Bernardino, O. Lam, A. Roussel, C. Amra, L. Escoubas, G. Albrand, and M. Commandré, "Characterization of optical coatings: damage threshold/local absorption correlation," in *Laser-Induced Damage in Optical Materials: 1996*, H. E. Bennett, A. H. Guenther, M. R. Kozlowski, B. E. Newnam, and M. J. Soileau, eds., Proc. SPIE 2966, 292-305 (1997).
8. R. J. Tench, R. Chow, M. R. Kozlowski, "Characterization of defect geometries in multilayer optical coatings", J. Vac. Sci. Technol. A **12**, 2808-2813 (1994).
9. C. J. Stolz, R. J. Tench, M. R. Kozlowski, and A. Fornier, "A comparison of nodular defect seed geometeries from different deposition techniques" in *Laser-Induced Damage to Optical Materials: 1995*, H. E. Bennett, A. H. Guenther, M. R. Kozlowski, B. E. Newnam, and M. J. Soileau, eds., Proc. SPIE 2714, 374-382 (1996).
10. E. Welsch, K. Ettrich, M. Peters, H. Blaschke, W. Ziegler, A. Bodemann, M. Reichling, "Application of photothermal probe beam deflection technique for the high-sensitive characterization of optical thin films with respect to their optical, thermal and thermoelastic inhomogeneities," in Optical Interference Coatings, F. Abelés, ed. Proc. SPIE 2253, 993-1004 (1994).
11. E. Welsch, M. Reichling, "Micrometer resolved photothermal displacement inspection of optical coatings", J. Mod. Opt. **40**, 1455-1475 (1993).
12. M. Reichling, E. Welsch, A. Duparré, E. Matthias, "Photothermal absorption microscopy of defects in ZrO_2 and MgF_2 single layer films", Optical Engineering **33**, 1334-1342 (1994).
13. E. Welsch and D. Ristau, "Photothermal measurements on optical thin films", Appl. Opt. **34**, 7239-7253 (1995).
14. M. Commandré and E. Pelletier, "Measurements of absorpion losses in TiO2 films by a collinear phototheramal deflection technique", Appl. Opt **29**, 4276-4283 (1990).
15. M. Commandré, P. Roche, "Characterization of optical coatings by photothermal deflection", Appl. Opt. **35**, 5012-5034 (1996).
16. A. Gatto and M. Commandré, "Multiscale mapping technique for the simultaneous estimation of absorption and partial scattering in optical coatings", Appl. Opt. **41**, 225-234 (2002).
17. Z. L. Wu, M. Reichling, X. Q. Hu, K. Balasubramanian, and K. H. Guenther, "Absorption and thermal conductivity of oxide thin films measured by photothermal displacement and reflectance methods", Appl. Opt. **32**, 5660-5665 (1993).
18. A. Dubois, A. C. Boccara, and M. Lebec, "Real-time reflectivity and topography imagery of depth-resolved microscopic surfaces," Optics Letters **24**, 309-311 (1999).
19. C. J. Stolz, F. Y. Genin, and T. V. Pistor "Electric-field enhancement by nodular defects in multilayer coatings irradiated at normal and 45° incidence", in *Laser-Induced Damage in Optical Materials: 2003*, G. J. Exarhos, A. H. Guenther, N. Kaiser, K. L. Lewis, M. J. Soileau, and C. J. Stolz, eds., in this proceedings.